Channelized Melting Drives Thinning Under a Rapidly Melting Antarctic Ice Shelf

Noel Gourmelen, Dan N. Goldberg, Kate Snow, Sian F. Henley, Robert G. Bingham, Satoshi Kimura, Anna E. Hogg, Andrew Shepherd, Jeremie Mouginot, Jan T. M. Lenaerts, et al.

AGU PUBLICATIONS

Geophysical Research Letters

RESEARCH LETTER
10.1002/2017GL074929

Key Points:
- High-resolution surface elevation change shows channelized thinning, unabated from the grounding line up to the calving front
- Thinning is related to channelized basal melting controlled by ocean circulation and cavity geometry
- Process has been ongoing for over 25 years, thinning the shelf to 3 quarter of its original height, making it more vulnerable to collapse

Supporting Information:
- Supporting Information S1

Correspondence to:
N. Gourmelen,
noel.gourmelen@ed.ac.uk

Citation:
Gourmelen, N., Goldberg, D. N., Snow, K., Henley, S. F., Bingham, R. G., Kimura, S., … van de Berg, W. J. (2017). channelized melting drives thinning under a rapidly melting Antarctic ice shelf. *Geophysical Research Letters*, *44*, 9796–9804. https://doi.org/10.1002/2017GL074929

Received 13 JUL 2017
Accepted 27 AUG 2017
Published online 10 OCT 2017

Channelized Melting Drives Thinning Under a Rapidly Melting Antarctic Ice Shelf

Noel Gourmelen[1,2], Dan N. Goldberg[1], Kate Snow[1], Sian F. Henley[1], Robert G. Bingham[1], Satoshi Kimura[3,4,8], Anna E. Hogg[5], Andrew Shepherd[5], Jeremie Mouginot[6], Jan T. M. Lenaerts[7], Stefan R. M. Ligtenberg[7], and Willem Jan van de Berg[7]

[1]School of GeoSciences, University of Edinburgh, Edinburgh, UK, [2]IPGS UMR 7516, Université de Strasbourg, CNRS, Strasbourg, France, [3]Nansen Center and Bjerknes Centre for Climate Research, Bergen, Norway, [4]British Antarctic Survey, Cambridge, UK, [5]Center for Polar Observation and Modelling, University of Leeds, Leeds, UK, [6]Department of Earth System Science, University of California, Irvine, CA, USA, [7]Institute for Marine and Atmospheric Research Utrecht, Utrecht University, Utrecht, Netherlands, [8]Japan Agency for Marine-Earth Science and Technology, Yokosuka, Japan

Abstract Ice shelves play a vital role in regulating loss of grounded ice and in supplying freshwater to coastal seas. However, melt variability within ice shelves is poorly constrained and may be instrumental in driving ice shelf imbalance and collapse. High-resolution altimetry measurements from 2010 to 2016 show that Dotson Ice Shelf (DIS), West Antarctica, thins in response to basal melting focused along a single 5 km-wide and 60 km-long channel extending from the ice shelf's grounding zone to its calving front. If focused thinning continues at present rates, the channel will melt through, and the ice shelf collapse, within 40–50 years, almost two centuries before collapse is projected from the average thinning rate. Our findings provide evidence of basal melt-driven sub-ice shelf channel formation and its potential for accelerating the weakening of ice shelves.

Plain Language Summary Ice shelves act as safety bands around the Antarctic ice sheet. Many ice shelves are currently thinning, leading to acceleration of the grounded ice behind. Here we show that ice shelves' thinning is stronger along a channel structure formed by the ocean circulation under the ice shelf. The thinning is 3 times higher than the ice shelf's average, hence leading to a more rapid weakening of the ice shelf. This study provides evidence of basal melt-driven sub-ice shelf channel formation and its potential for accelerating the weakening of ice shelves.

1. Introduction

The majority of meteoric ice that forms in West Antarctica leaves the ice sheet through floating ice shelves, many of which have been thinning substantially over the last 25 years (Holland et al., 2015; Paolo et al., 2015; Pritchard et al., 2012; Shepherd et al., 2003). A significant proportion of ice shelf thinning has been driven by submarine melting (Depoorter et al., 2013; Rignot et al., 2013; Shepherd et al., 2003) facilitated by increased access of relatively warm (>0.6°C) (Jacobs et al., 1996; Randall-Goodwin et al., 2015; Schofield et al., 2015) modified Circumpolar Deep Water (CDW) to subshelf cavities (Dutrieux et al., 2014). Ice shelves play a significant role in stabilizing the ice sheet from runaway retreat (de Angelis & Skvarca, 2003; Pritchard et al., 2012; Rott et al., 2002; Scambos et al., 2014; Shepherd et al., 2004) and regulating its contribution to sea level change (Shepherd et al., 2012). Ice shelf melting has also been implicated in sustaining high primary productivity (PP) in Antarctica's coastal seas (Arrigo et al., 2015) (Figure 1). However, these processes vary regionally and are not fully understood. Under some ice shelves, concentrated melting leads to the formation of inverted channels (Alley et al., 2016; Berger et al., 2017; Fricker et al., 2009; Le Brocq et al., 2013; Marsh et al., 2016; Rignot & Steffen, 2008; Sergienko, 2013). These channels guide buoyant melt-laden outflow, which can lead to localized melting of the sea ice cover (Mankoff et al., 2012). In extreme cases, the ice shelf is considerably thinner along the channels, with example of channels reducing the ice shelf thickness by half (Rignot & Steffen, 2008). The channels may potentially lead to heightened crevassing, which in turn affects ice shelf stability (Vaughan et al., 2012). Meanwhile, numerical studies suggest that buttressing loss is sensitive to the location of ice removal within an ice shelf (Fürst et al., 2015; Goldberg et al., 2012). Thus, it is important that we observe spatial patterns, as well as magnitudes, of ice shelf thinning, in order to improve understanding of the ocean drivers of thinning and of their impacts on ice shelf stability.

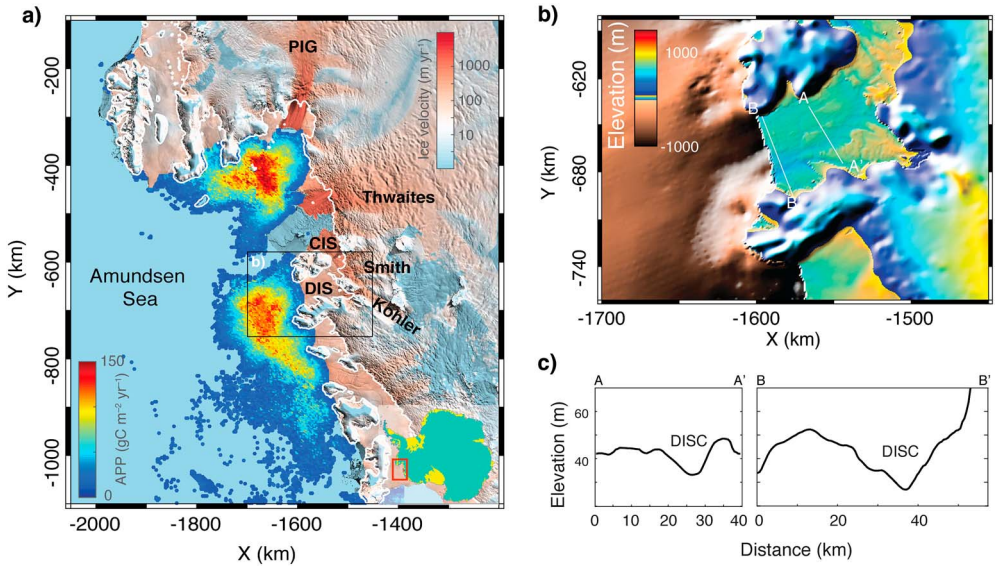

Figure 1. Dotson Ice Shelf, Amundsen Sea Sector; ice discharge, primary productivity, topography and bathymetry. (a) Ice flow of grounded ice across the grounding line (white line) feeding floating ice shelves (DIS and Crosson Ice Shelf (CIS)) and regions of high annual primary productivity (APP) (Arrigo et al., 2015). (b) Bathymetry and topography in the region of the DIS with the location of profiles (white lines) shown in Figure 1c; (c) DIS surface topography along the two profiles across DISC shown in Figure 1b—Ice flows out of page.

Dotson Ice Shelf (DIS) is a 70 km long by 50 km wide ice shelf in the Amundsen Sector of West Antarctica (Figure 1) which buttresses Kohler (KG) and Smith Glaciers (SG). In recent decades, KG and SG have exhibited significant thinning and retreat (Scheuchl et al., 2016). Between 1994 and 2012, DIS thinned at a constant rate of 2.6 m yr^{-1}, a rate 37% above the Amundsen Sea sector mean (Paolo et al., 2015), and ice discharge across the grounding line into the ice shelf increased by 180%, 30% above the Amundsen Sea sector mean (Mouginot et al., 2014). The surface ocean in front of DIS is cooled to the surface freezing point in the winter (Webber et al., 2017), and the upper ocean remains at or near the freezing point year round (Jacobs et al., 2011; Kim et al., 2017); but a deep trough traverses the continental shelf (Figure 1b), which facilitates CDW access to the subshelf cavity (Wåhlin et al., 2013), promoting high submarine melt rates. To date, only a handful of estimates of melt rates under Dotson have been made. An annually averaged submarine-melt rate of 7.8 ± 0.6 m yr^{-1} was inferred from satellite data for the period 2003–2008 (Rignot et al., 2013). At the grounding lines of KG, feeding DIS, melt rates of 40–70 m yr^{-1} have been inferred from airborne observations (Khazendar et al., 2016). Hydrographic estimates from January 2011 (Randall-Goodwin et al., 2015) suggested an ice removal rate of 81 Gt yr^{-1}—equivalent to a submarine-melt rate of ~15 m yr^{-1} using the same area baseline as the satellite estimate and an ice density of 917 kg m^{-3}. Meanwhile, a glider-based estimate from January 2014 (Miles et al., 2016) suggested ~3.5 m yr^{-1}. The latter two measurements were taken during the Austral summer, when melt rates are expected to be elevated and likely do not reflect the annual average. Importantly, none of the above results provide a detailed spatial pattern of melt and thus offer little capability for assessing the role of channels and small-scale features in defining basal melt concentration. This is important as understanding how Dotson Ice Shelf thins and is melted by the ocean is critical to predicting the future contribution to sea level of the grounded ice draining through Kohler and Smith glaciers.

2. Data and Methods

Regional-scale inferences of net melt at the ice shelf/ocean interface have relied on observations of ice shelf surface elevation change. The resolution of such net basal melting is largely constrained by the spatial resolution of the satellite altimetry measurements, which is on the order of tens of kilometers as a consequence of satellite track separations and instrument footprint size (Paolo et al., 2015; Shepherd et al., 2003) (Figure S1 in the supporting information).

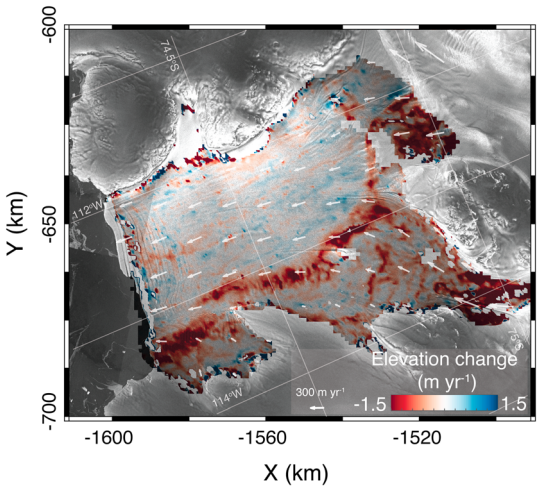

Figure 2. Rates of surface elevation change of the Dotson Ice Shelf. Lagrangian rates of surface elevation change between 2010 and 2016 from CryoSat-2 altimetry. Background shows Sentinel-1 radar images. Ice surface velocity is shown (white arrows).

In order to resolve elevation change at a spatial-scale commensurate with observed ice shelf channels, we generate a new elevation dataset using CryoSat-2 interferometric-swath radar altimetry acquired from 2010 to 2016 (Foresta et al., 2016). Swath processing leads to an order of magnitude higher spatial density than conventional radar altimetry techniques (i.e., Point-of-Closest-Approach), even over relatively flat topography found in ice shelves (Figure S1).

We then derive rates of surface elevation change $\dot{h}$ between 2010 and 2016 from the time-dependent swath elevation (Figure 2). We use a Lagrangian framework to derive $\dot{h}$ as to avoid interference of advecting ice shelf topography (Dutrieux et al., 2013; Moholdt et al., 2014). To this effect, we use ice velocity obtained from tracking of radar observation by the European Space Agency Sentinel-1a mission between 2013 and 2016 (Rignot et al., 2011; Rignot et al., 2017) (supporting information) to calculate and assign the position that each CryoSat-2 swath elevation measurements would have had at the beginning of the CryoSat-2 period, set at July 2010. The rates of surface elevation change and a Digital Elevation Model are then derived using a plane fit approach (Foresta et al., 2016) applied to the swath CryoSat-2 elevations. The map of linear rates of surface elevation change between 2010 and 2016, $\dot{h}$, and the swath Digital Elevation Model, c_2, is solved on a grid of 500 m posting. We use a simple bilinear model within each 500 m grid cell to describe the spatial variation of topography:

$$z(x, y, t) = c_0 x + c_1 y + \dot{h} t + c_2 \tag{1}$$

where z is the CryoSat-2 elevation, x, y, t are easting, northing, and time, respectively, c_0 and c_1 the topography slopes in the x and y direction, and c_2 the surface elevation at the cell center.

The chosen spatial resolution of 500 m allows observations at the length scales comparable to features associated with ice shelf melt variability of 500 m to 3 km (Alley et al., 2016; Dutrieux et al., 2013). We also quantify the change in ice velocity during the survey time period which, together with the digital elevation model (DEM), provide a measure of surface elevation change due to ice advection and ice divergence.

The melt rate of DIS is assessed through the following (Jenkins & Doake, 1991):

$$\dot{m} = \mathrm{SMB} - \left(\dot{h} + S\nabla\cdot\boldsymbol{u}\right)\cdot\frac{1}{1-\rho_{\mathrm{ice}}/\rho_{\mathrm{ocean}}} \tag{2}$$

where $\dot{m}$ is basal melt rate, SMB is the surface mass balance (van Wessem et al., 2016), ρ_{ice} is ice density of 917 kg m^{-3}, ρ_{ocean} nominal ocean density of 1,028 kg m^{-3}, $\boldsymbol{u}$ is velocity, S is surface elevation from the DEM, corrected for a 1.5 m penetration bias (Figure S3). All terms in the equation are contemporary; the ice velocity spans a slightly shorter period (2013–2016) than the other terms (2011–2016). Ice velocity differences between 2011 and 2013 are likely minimal since the Lagrangian treatment of the CryoSat elevation shows no advection residual; this suggest that the slight mismatch between ice velocity and the remainder of the balanced equation will have a negligible impact on the robustness of the calculated melt rates. A more detailed discussion of the methodology can be found in the supporting information (Arakawa & Lamb, 1977; Dehecq et al., 2015; Drews, 2016; Fretwell et al., 2013; Langley et al., 2014; Lenaerts et al., 2012; Ligtenberg et al., 2011; McMillan et al., 2011; Medley et al., 2013; Mouginot et al., 2012; Ng & King, 2011; Padman et al., 2002; Rignot et al., 2014; Timmermann et al., 2010; Trusel et al., 2013; Van Wessem et al., 2014; Zwally et al., 2012).

3. Results

The mean rate of surface elevation change for the whole of DIS between 2010 and 2016 is -0.26 ± 0.03 m yr^{-1}, which is consistent within errors with the rate of -0.28 ± 0.03 m yr^{-1} reported for 1994–2012 (Paolo et al., 2015). Strikingly, however, the finer resolution of our measurements enables us to discriminate parts of the DIS where the absolute rates are significantly larger, locally exceeding 1 m yr^{-1}. A feature, visible along the

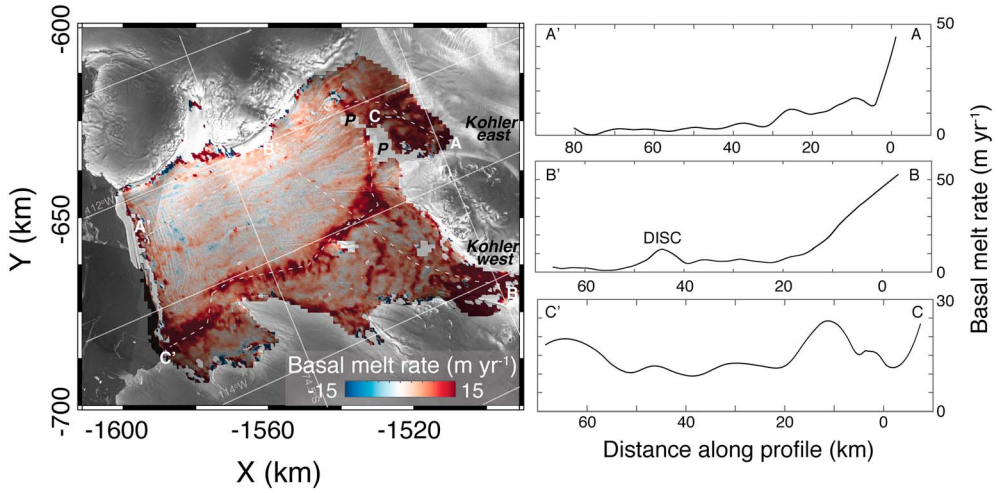

Figure 3. Total basal melt rates of the Dotson Ice Shelf. (left) Spatial distribution of basal melt rates, location of profiles indicated by dashed curves. The profiles show melt rates across the ice shelf from the Kohler east grounding line (A-A′) and Kohler west grounding line (B-B′), and along the DISC (C-C′). Location of pinning points (P) identified in text and Kohler east and Kohler west glaciers.

western edge of the DIS, consists of a quasi-continuous ~5 km-wide band of negative elevation change extending from the southern (landward) sector of the ice shelf to the ice shelf calving front (Figure 2). Along this feature, henceforth termed the DIS Channel (DISC), the mean rate of elevation change is -0.76 ± 0.03 m yr^{-1}, which accounts for 30% of the total elevation change of DIS.

Along the DISC, ice is significantly thinner than found elsewhere across the ice shelf, with surface elevation 10 to 20 m below the surrounding areas. The surface elevation depression is matched by a subshelf channel incised upward into the ice to between 100 and 200 m (supporting information S2). While much of the recent thinning of DIS has clearly been concentrated along the DISC, it is unknown for how long this process has formed a major component of the ice shelf's loss. From ice velocity measurements acquired in 2008, the DISC can be discerned as a region of broad ice convergence, suggesting that focused basal melting was already occurring there by 2008 (Rignot et al., 2013). Surface elevation change between 1991 and 2010, computed from lower spatial resolution radar altimetry (Figure S5), shows that the broad region around the DISC was lowering at rates of 0.5 m yr^{-1}, significantly faster than the remainder of DIS that was lowering at $<$0.1 m yr^{-1}. These indirect and sparse observations suggest that the localized thinning observed between 2010 and 2016 has been ongoing for at least two decades.

To elucidate the potential causes of the concentrated ice shelf thinning observed along the DISC, we considered various factors. A comparison of DIS's velocity structure in 2015 with that of 2008 (Figure S9) shows that changes in ice divergence could not be the cause of the observed signal in the altimetry data and hence that the observed surface lowering does not have an ice-dynamic origin. We also eliminate any explanation that invokes surface processes, because the magnitudes of changes related to surface processes are small here (Figure S8) and no evidence of surface melt has been recorded (Kingslake et al., 2017). We propose that the most likely explanation for the observed surface lowering is thinning caused by melting at the base of the ice shelf.

We find that basal melt is concentrated at the grounding line of KG east and KG west and along the DISC and that little melt occurs elsewhere under DIS (Figure 3). The total $\dot{m}$ under DIS amounts to an average basal melt of 6.1 $\pm$ 0.7 m yr^{-1}. The basal melting under the Kohler east and Kohler west grounding lines dominates the total basal melt budget, with rates of up to 50 m yr^{-1} (Figure 3), in agreement with values of 40 to 70 m yr^{-1} derived from local airborne surveys (Khazendar et al., 2016). Elsewhere in DIS, basal melt is concentrated along the DISC, averaging 14 m yr^{-1} (Figure 3). The channelized melt pattern is continuous, from the grounding zone of Kohler east to DIS's calving front. We observe continuous melt across a series of pinning points between Kohler east and DIS, indicating that this region of the DIS, near Kohler

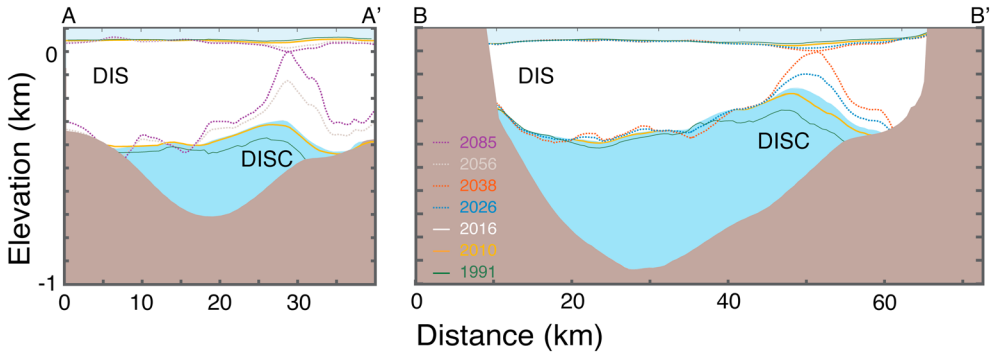

Figure 4. Observed and projected thickness evolution of the Dotson Ice Shelf. Between 2010 and 2016 DIS has lost an average of 7 m of ice along the DISC with very little thinning elsewhere with the exception of the KG grounding line. Elevation change from lower resolution observations between 1991 and 2010 (green solid line) show that thinning at DISC has been taking place over the last 25 years. Colored dashed lines are a simple projection of ice thickness across the channel (see Figure 1c for location) if current thinning rates were to persist.

east, is ungrounded at the time of our observations, supporting observation of ongoing grounding line retreat (Scheuchl et al., 2016).

4. Discussion

A large number of channels observed around Antarctica are thought to be driven by subglacial runoff (Drews et al., 2017; Le Brocq et al., 2013). However, the size of runoff-driven melt channels generated at the grounding lines is known to diminish with the distance from the grounding line (Drews, 2016; Dutrieux et al., 2014; Le Brocq et al., 2013). This is counter to our observations along the DISC showing sustained melt rate and thinning along the entire length of the channel (Figure 3). We therefore suggest that DISC is mainly the result of ocean forcing rather than related to subglacial or grounding line processes. This is in agreement with Alley et al. (2016), who classify the majority of sub-ice shelf channels in the Amundsen and Bellingshausen (including DISC) as "ocean sourced," as opposed to being driven by subglacial runoff (subglacially sourced). The authors attribute this to the extensive CDW on the continental shelf. It is generally thought that CDW enters DIS cavity by way of a trough at the ice shelf front (Wåhlin et al., 2013), though new estimates of bathymetry suggest a connection with Crosson Ice Shelf in the southeast corner of Dotson, near the Kohler East grounding line (Millan et al., 2017). Thus, it is conceivable that some of the forcing originates from the east, in Pine Island Bay.

Regardless of the CDW source, the location of the meltwater outflow is a straightforward consequence of ocean physics: warm water, originating at depth and becoming buoyant due to melt freshening, flows along the ice shelf bottom and is guided to the left by Coriolis forces. Ocean circulation and ice thinning then self-organize to yield the thinning pattern observed. Evidence of this process is given by the observation of elevated melt on the Coriolis-favored side of DISC (Figure S7) supporting the hypothesis that water flowing within DISC is deflected by Coriolis and thus is guided by the channel itself. This conceptual method of channel formation is distinct from that of subglacially sourced channels such as that observed in Roi Baudoin ice shelf (Drews et al., 2017), as the buoyant driver required for the high velocities that lead to amplified melt (Jenkins, 2011) comes from the melt itself, not the fresh subglacial runoff. This may be why the melt (and hence the channel) can persist to the ice shelf front, rather than diminishing with distance from the grounding line, and suggests that the presence of CDW is prerequisite for the DISC to exist.

We point out that to show conclusively that the location of DISC is a result of such self-organization would require sophisticated coupled ice-ocean modeling of DIS and its cavity. Modeling studies which have investigated coupled ice-ocean dynamics of idealized ice shelves forced by warm waters (Goldberg et al., 2012; Sergienko, 2013) have spontaneously yielded marginal melt-driven channels in absence of subglacial runoff, suggesting self-organization can occur.

Upon examination of transverse surface and basal profiles (Figures 1c, 4, and supporting information section S2), most profiles exhibit the asymmetry demonstrated by Alley et al. (2016) with the apex of melting

occurring on the Coriolis-favored side of the channel (Figure S7), which is thought to be caused by geostrophic "slumping" of the fast-flowing water to the Coriolis-favored side. The observed asymmetry is variable along the channel which is consistent with an ocean-sourced mechanism, a number of factors (e.g., water velocity, mixed layer depth, and steepness of the ice shelf base in the flow direction) govern the relative importance of the Coriolis force. Moreover, suggestion that asymmetry might be less strong where melting is higher (Dutrieux et al., 2013) could also explain the variability in observed asymmetry along the channel.

Our observations have implications for the stability of DIS. A simple forward projection using the currently observed pattern and rates of thinning leads to complete melt through of the DISC within 40 years (Figure 4); 170 years earlier than DIS would thin to zero using the ice shelf averaged thinning rate although considerable uncertainties are attached to this projection. While the forward projection of current rates of thinning implicitly takes into account current melting, advection, and dynamic thinning rates, it discounts the possibility that they will likely change as the ice thins, and it is known that a moderate acceleration of DIS flow is ongoing (McMillan et al., 2012; Mouginot et al., 2014). In this respect, the location of amplified thinning may be critical. Recent studies have shown that the stability of many ice shelves, as well as the response of grounded ice, is critically sensitive to buttressing at the shear margins (Borstad et al., 2013; Fürst et al., 2016; Goldberg et al., 2012), which can be limited by marginal thinning. Moreover, while deeply incised channels have been observed to nearly melt through ice shelves (Rignot & Steffen, 2008), additional processes could be taking place as DISC continues to thin and before it reaches complete melt through; amplified thinning along shear margins will lead to increased rates of crevassing, further weakening the buttressing ability of DIS and accelerating the potential for ice shelf collapse (Alley et al., 2016; Khazendar et al., 2007, 2011).

The extent to which the present thinning will sustain is also uncertain as the timing of the ocean perturbation that has led to the current imbalance is unknown. As indicated above, DIS has likely been melting out of balance for two decades or more. Numerical experiments suggest that an ice shelf exposed to persistent melt reaches an equilibrium on a time scale commensurate with the ice shelf residence time; i.e., the average time it takes for a column of ice to traverse the shelf (Goldberg et al., 2012; Little et al., 2012; Seroussi et al., 2017). For DIS this time scale is 50–100 years, suggesting that the high melt rates observed now originated in the twentieth century.

The prominence of localized, along-channel ice shelf thinning in the high-resolution satellite altimetry record across DIS has allowed us here to explore ocean-driven sub-ice shelf melting processes. Ice shelf thinning due to channelized ocean-sourced melting has seldom been observed across Antarctic ice shelves, likely not because the process is absent, but because the resolution of observations and complexities such as advection of complex topography makes it more difficult to identify. The increasing availability of high spatial resolution altimetry and of ice velocity observation at sufficient temporal resolution will greatly help the global identification of basal channelization under ice shelves. Episodic polynya formation at the fronts of other key ice shelves, such as at Pine Island Glacier (Mankoff et al., 2012), testifies to the existence of large subshelf channels elsewhere. Moreover, the ice shelf characteristics most key to the occurrence of ocean-driven channelized melting—exposure to intrusion of warm CDW and position in a semiclosed embayment—are common for a number of Antarctic ice shelves. It is therefore likely that the pattern and importance of melt-driven thinning along boundaries or shear margins of ice shelves we have identified here is widespread and is currently weakening ice shelves elsewhere around Antarctica.

5. Conclusions

We demonstrate that swath processing of CryoSat-2 data can lead to 1 order of magnitude increase in elevation measurement over ice shelves, providing the possibility to derive a unique set of global and detailed observations of time-dependent melt rates along ice shelves' channels. Using these high-resolution measurements of time-dependent elevation change, we show that channelized thinning has been taking place at the Dotson Ice Shelf between the years 2010 and 2016 and that out-of-balance thinning has likely been sustained for the last 25 years. Unlike observations at other ice shelves, we find here that channelized thinning is sustained from the grounding line up to the ice shelf's calving front and is caused by elevated basal melting located on the Coriolis-favored side of the channel forced by ocean circulation within the subshelf cavity. The subshelf channel incises 100 to 200 m into the shelf and exceeds in place the thickness of the ice

above; if current thinning rates persist, the channel would melt through by the end of the century. It is however likely that the ice shelf will respond to the imbalance before this occurs, potentially leading to an extension of the region of thinning, increased calving or potential collapse although the nature of this response is uncertain. Whatever the type of response, continued thinning and or collapse of DIS, it will lead to increase discharge of the grounded ice draining into the Dotson and Crosson ice shelves.

Acknowledgments
This work was supported by European Space Agency contracts CryoTop 4000107394/12/I-NB and CryoTop evolution 4000116874/16/I-NB (NG), a NERC grant NE/M003590/1 (D. G.), a NERC Independent Research Fellowship NE/K010034/1 (S. H.), an independent research fellowship 4000112797/15/I-SBo (A. H.) jointly funded by the European Space Agency, the University of Leeds and the British Antarctic Survey. We thank K. Arrigo, K. Lowry, and P. Jager for providing primary productivity data across the Amundsen Sea Sector. The CryoSat-2 satellite altimetry data are freely available from the European Space Agency (https://earth.esa.int/web/guest/data-access), and the specific data used in this study are provided within the supporting information. The IceBridge airborne altimetry data are freely available from the National Snow and Ice Data Centre (https://nsidc.org/data/icebridge/). The ice velocity data are freely available from the National Snow and Ice Data Centre (https://nsidc.org/data/nsidc-0484/). We are grateful to Reinhard Drews and an anonymous reviewer and the Editor, whose comments have significantly improved the manuscript.

References

Arakawa, A., & Lamb, V. R. (1977). Computational design of the basic dynamical processes of the UCLA general circulation model. In J. Chang (Ed.), *Methods in Computational Physics: Advances in Research and Applications* (Vol. 17, pp. 173–265). New York, Elsevier.

Alley, K. E., Scambos, T. A., Siegfried, M. R., & Fricker, H. A. (2016). Impacts of warm water on Antarctic ice shelf stability through basal channel formation. *Nature Geoscience*, *9*, 290–293.

Arrigo, K. R., van Dijken, G. L., & Strong, A. L. (2015). Environmental controls of marine productivity hot spots around Antarctica. *Journal of Geophysical Research: Oceans*, *120*, 5545–5565.

Berger, S., Drews, R., Helm, V., Sun, S., & Pattyn, F. (2017). Detecting high spatial variability of ice-shelf basal mass balance (Roi Baudouin ice shelf, Antarctica). *The Cryosphere Discussions*, *2017*, 1–22.

Borstad, C. P., Rignot, E., Mouginot, J., & Schodlok, M. P. (2013). Creep deformation and buttressing capacity of damaged ice shelves: Theory and application to Larsen C ice shelf. *The Cryosphere*, *7*, 1931–1947.

de Angelis, H., & Skvarca, P. (2003). Glacier surge after ice shelf collapse. *Science*, *299*, 1560–1562.

Dehecq, A., Gourmelen, N., & Trouve, E. (2015). Deriving large-scale glacier velocities from a complete satellite archive: Application to the Pamir–Karakoram–Himalaya, Remote Sens. *Environment*, *162*, 55–66.

Depoorter, M. A., Bamber, J. L., Griggs, J. A., Lenaerts, J. T. M., Ligtenberg, S. R. M., van den Broeke, M. R., & Moholdt, G. (2013). Calving fluxes and basal melt rates of Antarctic ice shelves. *Nature*, *502*, 89–92.

Drews, R. (2016). Evolution of ice-shelf channels in Antarctic ice shelves. *The Cryosphere*, *9*, 1169–1181.

Drews, R., Brown, J., Matsuoka, K., Witrant, E., Philippe, M., Hubbard, B., & Pattyn, F. (2016). Constraining variable density of ice shelves using wide-angle radar measurements. *The Cryosphere*, *10*, 811–823.

Drews, R., Pattyn, F., Hewitt, I. J., Ng, F. S. L., Berger, S., Matsuoka, K., … Neckel, N. (2017). Actively evolving subglacial conduits and eskers initiate ice shelf channels at an Antarctic grounding line. *Nature Communications*, *8*, 15,228.

Dutrieux, P., Vaughan, D. G., Corr, H. F. J., Jenkins, A., Holland, P. R., Joughin, I., & Fleming, A. H. (2013). Pine Island glacier ice shelf melt distributed at kilometre scales. *The Cryosphere*, *7*, 1543–1555.

Dutrieux, P., De Rydt, J., Jenkins, A., Holland, P. R., Ha, H. K., Lee, S. H., … Schröder, M. (2014). Strong sensitivity of Pine Island ice-shelf melting to climatic variability. *Science*, *343*, 174–178.

Foresta, L., Gourmelen, N., Pálsson, F., Nienow, P., Björnsson, H., & Shepherd, A. (2016). Surface elevation change and mass balance of Icelandic ice caps derived from swath mode CryoSat-2 altimetry. *Geophysical Research Letters*, *43*, 12,138–12,145. https://doi.org/10.1002/2016GL071485

Fretwell, P., Pritchard, H. D., Vaughan, D. G., Bamber, J. L., Barrand, N. E., Bell, R., … Zirizzotti, A. (2013). Bedmap2: Improved ice bed, surface and thickness datasets for Antarctica. *The Cryosphere*, *7*, 375–393.

Fricker, H. A., Coleman, R., Padman, L., Scambos, T. A., Bohlander, J., & Brunt, K. M. (2009). Mapping the grounding zone of the Amery Ice Shelf, East Antarctica using InSAR, MODIS and ICESat. *Antarctic Science*, *21*, 515–532.

Fürst, J. J., Durand, G., Gillet-Chaulet, F., Merino, N., Tavard, L., Mouginot, J., … Gagliardini, O. (2015). Assimilation of Antarctic velocity observations provides evidence for uncharted pinning points. *The Cryosphere*, *9*, 1427–1443.

Fürst, J. J., Durand, G., Gillet-Chaulet, F., Tavard, L., Rankl, M., Braun, M., & Gagliardini, O. (2016). The safety band of Antarctic ice shelves. *Nature Climate Change*, *6*, 479–482.

Goldberg, D. N., Little, C. M., Sergienko, O. V., Gnanadesikan, A., Hallberg, R., & Oppenheimer, M. (2012). Investigation of land ice-ocean interaction with a fully coupled ice-ocean model: 2. Sensitivity to external forcings. *Journal of Geophysical Research*, *117*, F02038. https://doi.org/10.1029/2011JF002247

Holland, P. R., Brisbourne, A., Corr, H. F. J., McGrath, D., Purdon, K., Paden, J., … Fleming, A. H. (2015). Oceanic and atmospheric forcing of Larsen C Ice-Shelf thinning. *The Cryosphere*, *9*, 1005–1024.

Jacobs, S. S., Hellmer, H. H., & Jenkins, A. (1996). Antarctic ice sheet melting in the Southeast Pacific. *Geophysical Research Letters*, *23*, 957–960.

Jacobs, S. S., Jenkins, A., Giulivi, C. F., & Dutrieux, P. (2011). Stronger ocean circulation and increased melting under Pine Island Glacier ice shelf. *Nature Geoscience*, *4*, 519–523.

Jenkins, A., & Doake, C. S. M. (1991). Ice-ocean interaction on Ronne Ice Shelf, Antarctica. *Journal of Geophysical Research*, *96*, 791–813.

Jenkins, A. (2011). Convection-driven melting near the grounding lines of ice shelves and tidewater glaciers. *Journal of Physical Oceanography*, *41*, 2279–2294.

Khazendar, A., Rignot, E., & Larour, E. (2007). Larsen B Ice Shelf rheology preceding its disintegration inferred by a control method. *Geophysical Research Letters*, *34*, L19503. https://doi.org/10.1029/2007GL030980

Khazendar, A., Rignot, E., & Larour, E. (2011). Acceleration and spatial rheology of Larsen C Ice Shelf, Antarctic Peninsula. *Geophysical Research Letters*, *38*, L09502. https://doi.org/10.1029/2011GL046775

Khazendar, A., Rignot, E., Schroeder, D. M., Seroussi, H., Schodlok, M. P., Scheuchl, B., … Velicogna, I. (2016). Rapid submarine ice melting in the grounding zones of ice shelves in West Antarctica. *Nature Communications*, *7*, 13,243.

Kim, T. W., Ha, H. K., Wåhlin, A. K., Lee, S. H., Kim, C. S., Lee, J. H., & Cho, Y. K. (2017). Is Ekman pumping responsible for the seasonal variation of warm circumpolar deep water in the Amundsen Sea? *Continental Shelf Research*, *132*, 38–48.

Kingslake, J., Ely, J. C., Das, I., & Bell, R. E. (2017). Widespread movement of meltwater onto and across Antarctic ice shelves. *Nature*, *544*, 349–352.

Langley, K., von Deschwanden, A., Kohler, J., Sinisalo, A., Matsuoka, K., Hattermann, T., … Isaksson, E. (2014). Complex network of channels beneath an Antarctic ice shelf. *Geophysical Research Letters*, *41*, 1209–1215. https://doi.org/10.1002/2013GL058947

Lenaerts, J. T. M., van den Broeke, M. R., van de Berg, W. J., van Meijgaard, E., & Kuipers Munneke, P. (2012). A new, high-resolution surface mass balance map of Antarctica (1979–2010) based on regional atmospheric climate modeling. *Geophysical Research Letters*, *39*, L04501. https://doi.org/10.1029/2011GL050713

Le Brocq, A. M., Ross, N., Griggs, J. A., Bingham, R. G., Corr, H. F. J., Ferraccioli, F., … Siegert, M. J. (2013). Evidence from ice shelves for channelized meltwater flow beneath the Antarctic Ice Sheet. *Nature Geoscience*, *6*, 945–948.
Ligtenberg, S. R. M., Helsen, M. M., & van den Broeke, M. R. (2011). An improved semi-empirical model for the densification of Antarctic firn. *The Cryosphere*, *5*, 809–819.
Little, C. M., Goldberg, D., Gnanadesikan, A., & Oppenheimer, M. (2012). On the coupled response to ice-shelf basal melting. *Journal of Glaciology*, *58*, 203–215.
Mankoff, K. D., Jacobs, S. S., Tulaczyk, S. M., & Stammerjohn, S. E. (2012). The role of Pine Island Glacier ice shelf basal channels in deep-water upwelling, polynyas and ocean circulation in Pine Island Bay. *Antarctic*, *53*, 23–28.
Marsh, O. J., Fricker, H. A., Siegfried, M. R., Christianson, K., Nicholls, K. W., Corr, H. F. J., & Catania, G. (2016). High basal melting forming a channel at the grounding line of Ross Ice Shelf, Antarctica. *Geophysical Research Letters*, *43*, 250–255. https://doi.org/10.1002/2015GL066612
McMillan, M., Shepherd, A., Nienow, P., & Leeson, A. (2011). Tide model accuracy in the Amundsen Sea, Antarctica, from radar interferometry observations of ice shelf motion. *Journal of Geophysical Research*, *116*, C11008. https://doi.org/10.1029/2011JC007294
McMillan, M., Shepherd, A., Gourmelen, N., Park, J. W., Nienow, P., Rinne, E., & Leeson, A. (2012). Mapping ice-shelf flow with interferometric synthetic aperture radar stacking. *Journal of Glaciology*, *58*, 265–277.
Medley, B., Joughin, I., Das, S. B., Steig, E. J., Conway, H., Gogineni, S., … Nicolas, J. P. (2013). Airborne-radar and ice-core observations of annual snow accumulation over Thwaites Glacier, West Antarctica confirm the spatiotemporal variability of global and regional atmospheric models. *Geophysical Research Letters*, *40*, 3649–3654. https://doi.org/10.1002/grl.50706
Miles, T., Lee, S. H., Wåhlin, A., Ha, H. K., Kim, T. W., Assmann, K. M., & Schofield, O. (2016). Glider observations of the Dotson Ice Shelf outflow. *Deep Sea Research Part II: Topical Studies in Oceanography*, *123*, 16–29.
Millan, R., Rignot, E., Bernier, V., Morlighem, M., & Dutrieux, P. (2017). Bathymetry of the Amundsen Sea Embayment sector of West Antarctica from Operation IceBridge gravity and other data. *Geophysical Research Letters*, *44*, 1360–1368. https://doi.org/10.1002/2016GL072071
Moholdt, G., Padman, L., & Fricker, H. A. (2014). Basal mass budget of Ross and Filchner-Ronne ice shelves, Antarctica, derived from Lagrangian analysis of ICESat altimetry. *Journal of Geophysical Research: Earth Surface*, *119*, 2361–2380. https://doi.org/10.1002/2016GL072071
Mouginot, J., Scheuchl, B., & Rignot, E. (2012). Mapping of ice motion in Antarctica using synthetic-aperture radar data. *Remote Sensing*, *4*, 2,753.
Mouginot, J., Rignot, E., & Scheuchl, B. (2014). Sustained increase in ice discharge from the Amundsen Sea Embayment, West Antarctica, from 1973 to 2013. *Geophysical Research Letters*, *41*, 1576–1584. https://doi.org/10.1002/2013GL059069
Ng, F., & King, E. C. (2011). Kinematic waves in polar firn stratigraphy. *Journal of Glaciology*, *57*, 1119–1134.
Padman, L., Fricker, H. A., Coleman, R., Howard, S., & Erofeeva, L. (2002). A new tide model for the Antarctic ice shelves and seas. *Annals of Glaciology*, *34*, 247–254.
Paolo, F. S., Fricker, H. A., & Padman, L. (2015). Volume loss from Antarctic ice shelves is accelerating. *Science*, *348*, 327–331.
Pritchard, H. D., Ligtenberg, S. R. M., Fricker, H. A., Vaughan, D. G., Van den Broeke, M. R., & Padman, L. (2012). Antarctic ice-sheet loss driven by basal melting of ice shelves. *Nature*, *484*, 502–505.
Randall-Goodwin, E., Meredith, M. P., Jenkins, A., Yager, P. L., Sherrell, R. M., Abrahamsen, E. P., … Stammerjohn, S. E. (2015). Freshwater distributions and water mass structure in the Amundsen Sea Polynya region, Antarctica. *Elementa: Science of the Anthropocene*, *3*, 65.
Rignot, E., & Steffen, K. (2008). Channelized bottom melting and stability of floating ice shelves. *Geophysical Research Letters*, *35*, L02503.
Rignot, E., Mouginot, J., & Scheuchl, B. (2011). Ice flow of the Antarctic ice sheet. *Science*, *333*, 1427–1430.
Rignot, E., Jacobs, S., Mouginot, J., & Scheuchl, B. (2013). Ice-shelf melting around Antarctica. *Science*, *341*, 266–270.
Rignot, E., Mouginot, J., Morlighem, M., Seroussi, H., & Scheuchl, B. (2014). Widespread, rapid grounding line retreat of Pine Island, Thwaites, Smith, and Kohler glaciers, West Antarctica, from 1992 to 2011. *Geophysical Research Letters*, *41*, 3502–3509. https://doi.org/10.1002/2014GL060140
Rignot, E., Mouginot, J., & Scheuchl, B. (2017). MEaSUREs InSAR-based Antarctica ice velocity map, Version 2. Boulder, Colorado USA. NASA National Snow and Ice Data Center Distributed Active Archive Center. https://doi.org/10.5067/D7GK8F5J8M8R, NASA National Snow and Ice Data Center Distributed Active Archive Center.
Rott, H., Rack, W., Skvarca, P., & de Angelis, H. (2002). Northern Larsen ice shelf, Antarctica: Further retreat after collapse. *Annals of Glaciology*, *34*, 277.
Scambos, T. A., Berthier, E., Haran, T., Shuman, C. A., Cook, A. J., Ligtenberg, S. R. M., & Bohlander, J. (2014). Detailed ice loss pattern in the northern Antarctic Peninsula: Widespread decline driven by ice front retreats. *The Cryosphere*, *8*, 2135–2145.
Scheuchl, B., Mouginot, J., Rignot, E., Morlighem, M., & Khazendar, A. (2016). Grounding line retreat of Pope, Smith, and Kohler Glaciers, West Antarctica, measured with Sentinel-1a radar interferometry data. *Geophysical Research Letters*, *43*, 8572–8579. https://doi.org/10.1002/2016GL069287
Schofield, O., Miles, T., Alderkamp, A., Lee, S., Haskins, C., Rogalsky, E., … Yager, P. L. (2015). *In situ phytoplankton distributions in the Amundsen Sea Polynya measured by autonomous gliders*. Elementa: Science of the Anthropocene.
Sergienko, O. V. (2013). Basal channels on ice shelves. *Journal of Geophysical Research: Earth Surface*, *118*, 1342–1355. https://doi.org/10.1002/jgrf.20105
Seroussi, H., Nakayama, Y., Larour, E., Menemenlis, D., Morlighem, M., Rignot, E., & Khazendar, A. (2017). Continued retreat of Thwaites Glacier, West Antarctica, controlled by bed topography and ocean circulation. *Geophysical Research Letters*, *44*, 6191–6199. https://doi.org/10.1002/2017GL072910
Shepherd, A., Wingham, D., Payne, T., & Skvarca, P. (2003). Larsen ice shelf has progressively thinned. *Science*, *302*, 856–859.
Shepherd, A., Wingham, D., & Rignot, E. (2004). Warm ocean is eroding West Antarctic Ice Sheet. *Geophysical Research Letters*, *31*, L23402 DOI: https://doi.org/10.1029/2004GL021106
Shepherd, A., Ivins, E. R., Geruo, A., Barletta, V. R., Bentley, M. J., Bettadpur, S., … Jay Zwally, H. (2012). A reconciled estimate of ice-sheet mass balance. *Science*, *338*, 1183–1189.
Timmermann, R., Le Brocq, A., Deen, T., Domack, E., Dutrieux, P., Galton-Fenzi, B., … Smith, W. H. F. (2010). Antarctic ice sheet topography, cavity geometry, and global bathymetry (RTopo 1.0.5-beta), Supplement to: Timmermann, R. et al. (2010): A consistent dataset of Antarctic ice sheet topography, cavity geometry, and global bathymetry. *Earth System Science Data*, *2*(2), 261–273. https://doi.org/10.5194/essd-2-261-2010
Trusel, L. D., Frey, K. E., Das, S. B., Munneke, P. K., & van den Broeke, M. R. (2013). Satellite-based estimates of Antarctic surface meltwater fluxes. *Geophysical Research Letters*, *40*, 6148–6153. https://doi.org/10.1002/2013GL058138
Van Wessem, J. M., Reijmer, C. H., Morlighem, M., Mouginot, J., Rignot, E., Medley, B., … Van Meijgaard, E. (2014). Improved representation of East Antarctic surface mass balance in a regional atmospheric climate model. *Journal of Glaciology*, *60*, 761–770.

van Wessem, J. M., Ligtenberg, S. R. M., Reijmer, C. H., van de Berg, W. J., van den Broeke, M. R., Barrand, N. E., … van Meijgaard, E. (2016). The modelled surface mass balance of the Antarctic Peninsula at 5.5 km horizontal resolution. *The Cryosphere*, *10*, 271–285.

Vaughan, D. G., Corr, H. F. J., Bindschadler, R. A., Dutrieux, P., Gudmundsson, G. H., Jenkins, A., … Wingham, D. J. (2012). Subglacial melt channels and fracture in the floating part of Pine Island Glacier, Antarctica. *Journal of Geophysical Research*, *117*, F03012. https://doi.org/10.1029/2012JF002360

Wåhlin, A. K., Kalén, O., Arneborg, L., Björk, G., Carvajal, G. K., Ha, H. K., … Stranne, C. (2013). Variability of warm deep water inflow in a submarine trough on the Amundsen Sea shelf. *Journal of Physical Oceanography*, *43*, 2054–2070.

Webber, B. G. M., Heywood, K. J., Stevens, D. P., Dutrieux, P., Abrahamsen, E. P., Jenkins, A., … Kim, T. W. (2017). Mechanisms driving variability in the ocean forcing of Pine Island Glacier. *Nature Communications*, *8*, 14,507.

Zwally, H. J., Giovinetto, M. B., Beckley, M. A., & Saba, J. L. (2012). Antarctic and Greenland Drainage Systems, GSFC Cryospheric Sciences Laboratory.